

Photoluminescence of p -doped quantum wells with strong spin splittingP. Kossacki,^{1,2,3,*} H. Boukari,¹ M. Bertolini,¹ D. Ferrand,¹ J. Cibert,^{1,4} S. Tatarenko,¹ J. A. Gaj,²
B. Deveaud,³ V. Ciulin,³ and M. Potemski⁵¹*Groupe "Nanophysique et Semiconducteurs," CEA-CNRS-Université Joseph Fourier Grenoble, Laboratoire de Spectrométrie Physique, BP87, F-38402 Saint Martin d'Hères Cedex, France*²*Institute of Experimental Physics, Warsaw University, Hoża 69, PL-00-681 Warszawa, Poland*³*Institute of Quantum Electronics and Photonics, Ecole Polytechnique Fédérale de Lausanne (EPFL), CH-1015 Lausanne, Switzerland*⁴*Laboratoire Louis Néel, CNRS, BP166, F-38042 Grenoble Cedex 9, France*⁵*Grenoble High Magnetic Field Laboratory, MPI-FKF/CNRS, 25 Avenue des Martyrs, F-38042 Grenoble Cedex 9, France*

(Received 10 April 2004; revised manuscript received 16 August 2004; published 23 November 2004)

The spectroscopic properties of a spin-polarized two-dimensional hole gas are studied in modulation doped $\text{Cd}_{1-x}\text{Mn}_x\text{Te}$ quantum wells with variable carrier density up to $5 \times 10^{11} \text{ cm}^{-2}$. The giant Zeeman effect, which is characteristic of diluted magnetic semiconductors, induces a significant spin splitting even at very small values of the applied field. Several methods of measuring the carrier density (Hall effect, filling factors of the Landau levels at high field, various manifestations of Moss-Burstein shifts) are described and calibrated. The value of the spin splitting needed to fully polarize the hole gas shows a strong enhancement of the spin susceptibility of the hole gas due to the carrier-carrier interaction. At small values of the spin splitting, whatever the carrier density (nonzero) is, photoluminescence lines are due to the formation of charged excitons in the singlet state. Spectral shifts in photoluminescence and in transmission (including an "excitonic Moss-Burstein shift") are observed and discussed in terms of excitations of the partially or fully polarized hole gas. At large spin splitting, and without changing the carrier density, the singlet state of the charged exciton is destabilized in favor of a triplet state configuration of holes. The binding energy of the singlet state is thus measured and found to be independent of the carrier density (in contrast to the splitting between the charged exciton and the neutral exciton lines). The state stable at large spin splitting is close to the neutral exciton at low carrier density, and close to an uncorrelated electron-hole pair at the largest values of the carrier density achieved. The triplet state gives rise to a characteristic double-line structure with an indirect transition to the ground state (with a strong phonon replica) and a direct transition to an excited state of the hole gas.

DOI: 10.1103/PhysRevB.70.195337

PACS number(s): 78.55.Et, 75.50.Pp, 75.30.Hx, 75.50.Dd

I. INTRODUCTION

The spectroscopy of two-dimensional (2D) systems with carriers has been studied intensively during past years. At low carrier density, optical spectra are dominated by a line related to the charged exciton (trion) transition.¹ In the limit of very low carrier density, the charged exciton is a three-particle complex involving a preexisting carrier and the photo-created electron-hole pair, the two identical particles being arranged in a singlet configuration. Some trion properties are well understood. For example, many papers were devoted to theoretical and experimental studies on the binding energy under different conditions and in different materials.²⁻⁶ Detailed investigations were also performed on the selection rules⁷⁻⁹ and on the dynamics,^{10-12,16} in particular the formation time¹³⁻¹⁵ and spin relaxation.^{11,17} Most of those properties are well established and can be used for identification purposes.

In high magnetic field, a triplet state has been described¹⁸⁻²⁰ and its stability with respect to the singlet state has been discussed in terms of orbital wave functions. The range of higher carrier densities is less understood. As the carrier density increases, an increase of the energy splitting between the absorption lines of the charged and neutral exciton has been reported in various materials.^{2,21-23} This effect does not necessarily mean that the binding energy changes: it is important to analyze both the initial and final states in-

involved in the spectroscopic transitions as well as the change of line shapes versus carrier density. Thus, recoil gives rise to low-energy tails while exciton-electron unbound states cause a strong high-energy tail, which adds a large contribution to the oscillator strength of the neutral exciton.²⁴⁻²⁶ At even higher densities, the neutral exciton line disappears and the charged exciton line progressively transforms into the Fermi edge singularity, which marks the onset of the electron-hole continuum.^{23,27,28} All these effects point to a non-negligible interaction of the charged exciton with the carrier gas.

We wish to discuss here selected problems related to the photoluminescence (PL) of doped quantum wells (QW's), thanks to new experimental results associated to a strong spin splitting in magnetic fields small enough to prevent Landau quantization. This is obtained thanks to the giant Zeeman effect in $\text{Cd}_{1-x}\text{Mn}_x\text{Te}$ QW's, which are modulation-doped p type. The carrier density was adjusted through the design of the structure using either nitrogen acceptors or surface states, and in some samples it was controlled either optically or through a bias applied across a p - i - n diode. A thorough calibration of the carrier density was done.

We show that for small values of the spin splitting ($< 3 \text{ meV}$), the PL line in both circular polarizations is due to the singlet state of the charged exciton. However, a shift appears between the absorption and PL lines^{23,29} and increases with the carrier density quite similarly to the Moss-

TABLE I. Characteristics of selected samples. Samples with “N” are doped using nitrogen acceptors on both sides of the QW, samples with “S” are doped from surface states, and samples with “D” are *p-i-n* diodes; numbers were chosen to approximately match the Mn content.

Sample	QW thickness (nm)	QW Mn content (%)	Max. hole density (10^{11} cm^{-2})	Structure	Growth name	Figure
N0	8	none	0.3	N-doped	M751	1
N2	8	0.18	3.1	N-doped	M968	3, 4(a), and 9(a)
N3	8	0.37	4.2	N-doped	M1038	5, 6, and 14
N4	8	0.40	3.2	N-doped	M1305	7, 8, 10, 11, and 13–15
N5	8	0.53	3.8	N-doped	M1132	2, 4(b), 9(b), 14, and 15
N4b	8	0.4	5.2	N-doped	M1131	14
S7	10	0.7	2.8	Surface doped	M1269	13–15
S8	10	0.7	1.5	Surface doped	M1290	14 and 15
D3	8	0.3	2.8	<i>p-i-n</i> diode	M1329	14 and 15
D50	8	5	1.8	<i>p-i-n</i> diode	M1346	14

Burstein shift of band-to-band transitions. This shift is discussed in terms of excitations in the final states of the transitions. It vanishes in σ^- polarization when the spin splitting is large enough that the hole gas be completely polarized: the relevant value of the spin splitting is discussed with respect to the Fermi energy.

Then, above a certain value of the spin splitting, the lowest initial state in the PL transition is no more the singlet state of the charged exciton, but a state where all holes are in the majority spin subband. That means that the singlet arrangement of the two holes involved in the charged exciton is replaced by a parallel arrangement of their spins (triplet state). Contrary to the case of nonmagnetic quantum wells, for which the triplet state of the charged exciton is stabilized by orbital effects at very high magnetic field,^{19,30,31} in the present case the singlet state is destabilized by spin effects. This gives rise to several features that agree with a mechanism involving band-to-band transitions (double line, with the lower component having the ground state of the hole gas as its final state and the upper one leaving the carrier gas in an excited state; and existence of a Moss-Burstein shift). Finally, different energy scales involved are discussed with reference to the Fermi energy.

This paper is organized as follows. Section II briefly describes the samples and the experimental setup. Section III is devoted to an advanced characterization of the samples and of the mechanisms involved in the spectroscopic properties, based on our previous knowledge of *p*-doped $\text{Cd}_{1-x}\text{Mn}_x\text{Te}$ QW's: determination of the diamagnetic shift and of the normal Zeeman effect, measurement of the giant Zeeman effect and derivation of the exact density of free spins, behavior at large values of the applied magnetic field, derivation of the position of the Landau levels and of the carrier density from the filling factors, and finally determination of the carrier density from Hall effect. Section IV is the core section of this paper: it describes the PL spectra that characterize a $\text{Cd}_{1-x}\text{Mn}_x\text{Te}$ QW in the presence of holes, first in the low-density limit where the spectra can be understood from the competition between neutral and charged excitons, then at higher carrier density where new features are observed and

analyzed in terms of the initial and final states involved in the PL transition and used to further characterize the hole gas (density and polarization). Some consequences of the observation of these new features are discussed in Sec. V.

II. SAMPLES AND EXPERIMENTAL SETUP

Samples have been grown by molecular-beam epitaxy from CdTe, ZnTe, Te, Cd, Mg, and Mn sources, on (001)-oriented $\text{Cd}_{1-z}\text{Zn}_z\text{Te}$ substrates, most of them with $z=0.12$, with a buffer layer of similar composition and (Cd,Zn,Mg)Te barriers. Characteristics of selected samples are summarized in Table I. All samples were grown pseudomorphically; therefore the lattice constant of the substrate governs the uniaxial strain in the single QW: due to confinement and strain, the heavy-hole state is the ground state in the valence band, the light-hole band being 30 to 40 meV higher in energy.

Most samples were modulation doped with nitrogen in the barriers.³² In others, the hole gas was provided by proper adjustment of the (Cd,Mg)Te cap layer thickness, with surface states playing the role of acceptors; our previous studies³³ allowed us to optimize the structure of these samples in order to obtain the largest hole density, by placing the QW 25 nm below the surface and 200 nm away from the (Cd,Zn)Te buffer layer. In both cases, illumination with light of energy larger than the energy gap of the barrier material results in the depletion of the hole gas:^{23,34,35} This method with a suitable calibration²³ was used in order to tune the carrier density in the QW from the maximum value (a few 10^{11} cm^{-2}) down to the low 10^{10} cm^{-2} range.

The second way to control the carrier concentration was to insert the QW in a *p-i-n* diode. In such a structure,³⁶ the back barrier doped with aluminum (*n* type) was 320 nm away from the QW, and the spacer between the QW and the *p*-doped layer was reduced to 10 nm. A 10 nm semitransparent gold film was evaporated on top of the *p-i-n* diodes, and then $2 \times 2 \text{ mm}^2$ squares were formed by Ar-ion etching down to the *n*-type layer, a procedure followed by the deposition of In contacts. In these diodes, nonlinear current-

voltage characteristics were observed up to room temperature, and applying a small bias resulted in variations of the carrier density from below 10^{10} cm^{-2} up to 4×10^{11} cm^{-2} . In all samples the hole densities are such that the carriers occupy only the ground-state heavy-hole subband.

All properties discussed below were determined or checked by magneto-optical spectroscopy performed in the Faraday configuration (magnetic field and light propagation perpendicular to the sample surface). The samples were mounted strain-free in a superconducting magnet and immersed in liquid helium for low-temperature measurements. The experimental setup allowed us to perform typical cw measurements such as reflectivity, PL, and PL excitation (PLE). The $\text{Cd}_{0.88}\text{Zn}_{0.12}\text{Te}$ substrates are transparent at the relevant wavelengths so that in most cases we could also perform transmission experiments. In PL, the optical excitation was achieved with a tunable Ti-sapphire laser providing about 2 mW cm^{-2} , or a HeNe laser with similar intensity. A halogen lamp (filtered to avoid carrier depletion, or not in order to induce a depletion) was used as a source of light for reflectivity and transmission measurements. Time-resolved PL was excited by a picosecond tunable Ti-sapphire laser with a 2 ps pulse width, a repetition rate of 80 MHz, and an averaged power density less than 100 mW cm^{-2} . The signal was collected through a spectrometer by a 2D streak camera with resolution better than 10 ps. The measurements in high magnetic fields were performed in the Grenoble High Field Laboratory using a 20 T Bitter coil.

III. BASIC SPECTROSCOPIC PROPERTIES AND CHARACTERIZATION OF THE 2D HOLE GAS

In this section we summarize the characterization of our samples and of some of their spectroscopic properties, based on the previous knowledge of undoped and *p*-doped CdTe and $\text{Cd}_{1-x}\text{Mn}_x\text{Te}$ QW's. We first determine the parameters describing the properties of the excitons under the direct influence of an applied magnetic field (diamagnetic shift, Landé factor) in a nonmagnetic CdTe QW. Then we show that by exploiting the giant Zeeman effect we achieve a good description of the excitons in a diluted magnetic QW at low hole density. Finally we turn to a thorough determination of the hole density, using methods that do not depend on materials parameters, such as plotting the positions of integer filling factors of Landau levels, or deriving the density from the Hall resistance.

A. Excitonic regime: Normal Zeeman effect and diamagnetic shift

Figure 1(a) shows typical transmission spectra measured at different values of the magnetic field on sample N0, which is a 8 nm thick CdTe QW, moderately doped *p* type (nitrogen doping on both sides with 50 nm spacer layers). The whole structure (QW, $\text{Cd}_{0.69}\text{Zn}_{0.08}\text{Mg}_{0.23}\text{Te}$ barriers, $\text{Cd}_{0.88}\text{Zn}_{0.12}\text{Te}$ buffer layer) is coherently strained on the $\text{Cd}_{0.88}\text{Zn}_{0.12}\text{Te}$ substrate, so that the light-hole–heavy-hole splitting is about 40 meV. At zero field, two lines are observed. As confirmed below, the higher-energy line is related to the neutral exciton

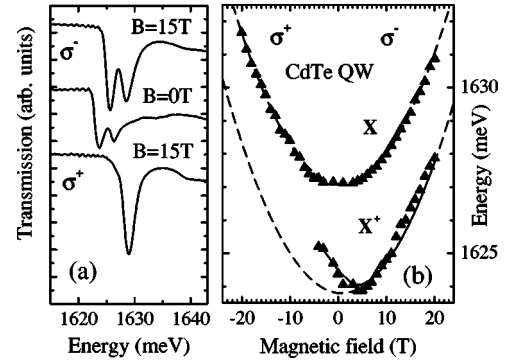


FIG. 1. (a) Typical transmission spectra and (b) magnetic field dependence of the transition energies, observed at 1.9 K on sample N0, an 8 nm broad CdTe QW with $\text{Cd}_{0.69}\text{Zn}_{0.08}\text{Mg}_{0.23}\text{Te}$ barriers, moderately doped *p*-type (two symmetrical N-doped layers at 50 nm). In (b), the right part (positive fields) displays the σ^- polarization data and the left part (negative fields) the σ^+ ones. Dashed lines are quadratic fits; the solid line through the charged-exciton positions is obtained when taking into account the dependence of the X/X^+ splitting on the hole polarization.

and the lower-energy one to a charged exciton. Under magnetic field, the neutral exciton is observed in both polarizations, while the low-energy line progressively disappears in σ^+ polarization. This behavior is opposite to that of the negatively charged exciton X^- , so that it was attributed to the positively charged exciton in Ref. 37, as confirmed and discussed quantitatively in the following.

Figure 1(b) shows the magnetic field dependence of the transition energies. By convention, we attribute positive field range to the σ^- polarization. The neutral exciton energy follows a quadratic dependence:

$$E_{\sigma_{\pm}} = E_X \mp a_z |B| + a_{dia} B^2$$

with $E_X = 1627 \text{ meV}$ in the present sample, $a_z = 0.015 \text{ meV T}^{-1}$, and $a_{dia} = 0.01057 \text{ meV T}^{-2}$. This value of the diamagnetic shift is reasonable: it corresponds to an effective radius of 6 nm, which is of the order of the Bohr radius.

Note the small value of the Zeeman shift (the linear term): defining the excitonic Landé factor as

$$g_X = \frac{E(\sigma^+) - E(\sigma^-)}{\mu_B |B|}$$

we have $g_X = 0.5$, definitely smaller than in CdTe QW's of similar width but with no strain³⁸ or a small one.³⁹ Indeed, in unstrained QW's the excitonic Landé factor $g_X = -1.5$ mostly corresponds to the Landé factor of the electron $g_e = -1.4$ (to be compared to $g_e = -1.6$ in bulk CdTe), indicating an almost vanishing Zeeman splitting in the valence band. In the present samples, coherently strained on the $\text{Cd}_{0.88}\text{Zn}_{0.12}\text{Te}$ substrate, using the same value $g_e = -1.4$ and our experimental value $g_X = 0.5$, we obtain $g_{hh} = g_X + g_e = -0.9$. We use here the spin Landé factor of the holes, i.e., the splitting between the two components of the heavy holes is $g_{hh} \mu_B B$. This finite Zeeman splitting of heavy holes is consistent with the magnetic circular dichroism of the trion, opposite to that of the

negatively charged exciton in n -type CdTe QW's. Indeed, in similar samples with a low hole density (in the 10^{10} cm^{-2} range) showing well defined excitonic lines, we could directly estimate $g_{hh} = -1.2$ from the field and temperature dependence of the dichroism by assuming that the distribution of carriers on the two spin states obeys the Maxwell-Boltzmann statistics and that the trion intensity in σ^- polarization is proportional to the density of $|+\frac{3}{2}\rangle$ holes.³⁷

The transition energy of the charged exciton in σ^- polarization above 4 T obeys the same dependence as the neutral exciton (with a diamagnetic shift at most 5% larger), 3.4 meV lower in energy. This value indicates a moderate but significant density of carriers, in the 10^{10} cm^{-2} range, if we compare to values measured in (Cd,Mn)Te QW's.²³ It was demonstrated there that the $X-X^+$ splitting in absorption contains a contribution proportional to the density of the hole gas in one spin subband (the one promoting the trion formation). We use this result in order to describe the behavior of the trion in the present CdTe QW below 4 T and in σ^+ polarization, where a shift to high energy is observed. At 3–4 T in σ^+ polarization, the binding energy tends to 2.0 meV, which is the value expected at vanishingly small population of the holes with the relevant spin. The solid line represents the fit with the $X-X^+$ splitting equal to 2.0 meV plus a term proportional to the hole gas density in the relevant spin subband. The spin polarization was calculated using the Maxwell-Boltzmann distribution between the Zeeman-split hole levels (with $g_{hh} = -1.2$). We obtain perfect agreement, which is an additional support for our identification of the two lines.

The values of the Zeeman splitting and diamagnetic shifts determined here will be used systematically in the following for excitonic states in DMS QW's, where the additional giant Zeeman effect is dominant.

B. Giant Zeeman effect

The parameters describing the giant Zeeman effect are easiest to determine on spectra obtained with above-barrier illumination so that the hole density is reduced. Figure 2 is an example of the position of the lines observed in transmission with additional Ar-ion laser light shining on the surface of sample N5 (with 0.53% Mn in the QW). Due to the residual hole gas, we observe the neutral exciton in σ^+ polarization and the positively charged exciton in σ^- polarization; the neutral exciton is also observed at high field (much stronger than the field for filling factor $n=1$) in σ^- polarization: this agrees with previous observations at high field in the presence of an electron gas.^{40,41}

The field dependence of both the neutral and charged exciton energies was fitted by adding the contribution from the giant Zeeman effect to the normal Zeeman effect and diamagnetic shift, with parameters from Ref. 42:

$$E_{\sigma^\pm} = E_X \mp a_z B + a_{dia} B^2 \mp N_0 (\alpha - \beta) \frac{5}{2} x_{eff} \mathbf{B}_{5/2} \left(\frac{\frac{5}{2} g_{Mn} \mu_B B}{k_B (T + T_0)} \right)$$

where the parameters a_z and a_{dia} were determined above, $\mathbf{B}_{5/2}$ denotes the Brillouin function, T the temperature, $N_0 \alpha$

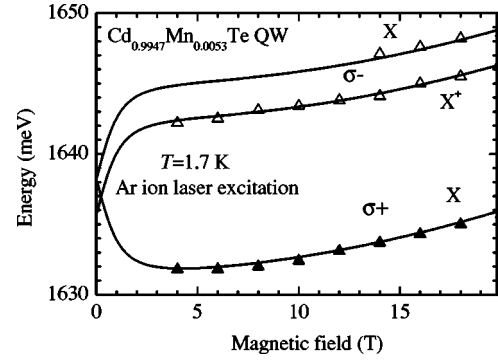


FIG. 2. Energy of the transmission line, as a function of applied field, at 1.7 K, for sample N5, a p -doped, 8 nm wide, $\text{Cd}_{1-x}\text{Mn}_x\text{Te}$ QW. Ar-ion laser illumination strongly reduces the carrier density to the low 10^{10} cm^{-2} range. Solid lines are drawn with the same parameters as in Fig. 1 to describe the normal Zeeman effect and diamagnetic shift, and a Brillouin function with $x_{eff} = 0.0048$ (and $x = 0.0052$, $T_0 = 0.17 \text{ K}$) to describe the giant Zeeman effect, and adjustable values for the zero-field energies of X and X^+ .

$= 0.22 \text{ eV}$ and $N_0 \beta = -0.88 \text{ eV}$ describe the spin-carrier coupling in the conduction and the valence band, respectively. The fitting parameter x_{eff} (density of free spins) and T_0 are related to the Mn content x by the following expressions, calculated from Ref. 42:

$$x_{eff} = x [0.2635 \exp(-43.34x) + 0.729 \exp(-6.190x) + 0.00721]$$

and

$$T_0 = \frac{35.37x}{1 + 2.752x} \text{ K.}$$

We did not include magnetization steps that are expected at high field and very low temperature^{43,44} and that would induce an additional linear increase of the magnetization at the temperatures of interest in the present study. The Mn content in our QW's remains below 1%, so that the amplitude of the steps remains small.

Mn contents quoted below are determined from the fit of the giant Zeeman effect. They were found to agree with those expected from growth conditions.

C. High-field Landau levels

Figure 3 displays transmission spectra of sample N2, i.e., a $\text{Cd}_{0.9982}\text{Mn}_{0.0018}\text{Te}$ QW with $\text{Cd}_{0.66}\text{Mg}_{0.27}\text{Zn}_{0.07}\text{Te}$ barriers doped p type on one side with a 20 nm spacer. In these spectra, the smooth rise of the background at high energy is due to absorption in the $\text{Cd}_{0.88}\text{Zn}_{0.12}\text{Te}$ substrate. At zero field, one observes an asymmetric absorption feature, as expected in the presence of a significant density of carriers. In this sample, in spite of the low Mn content, the giant Zeeman effect is large enough that the hole gas is fully polarized already at $B = 0.6 \text{ T}$;²³ as a result, circularly polarized spectra differ qualitatively.

With applied field, the σ^- spectra [Fig. 3(b)] feature mostly a single, intense line. The intensity of this line in-

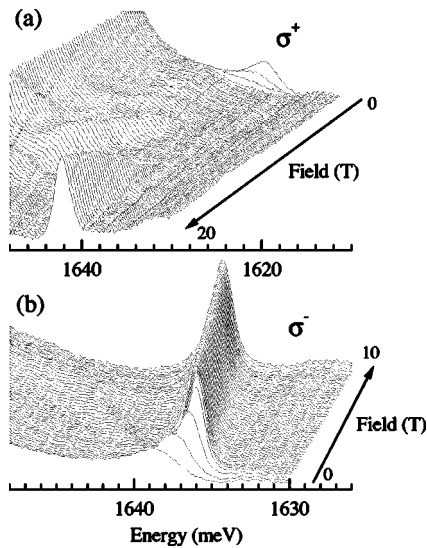


FIG. 3. (a) Optical density spectra obtained from transmission, at 1.7 K and magnetic fields from 0 to 20 T, in σ^+ polarization, for a $\text{Cd}_{0.9982}\text{Mn}_{0.0018}\text{Te}$ QW (sample N2); spectra have been shifted in both directions to enhance the principal features; (b) same as (a), in σ^- polarization, from 0 to 10 T; shifts are different in order to enhance the features of interest.

increases first (up to 0.6 T) as the hole gas becomes more and more polarized, so that the density of holes on the spin subband involved in the transition ($|\frac{3}{2}\rangle$ heavy holes) decreases to zero; then the intensity stays practically constant up to 10 T [Fig. 3(b)] and even 20 T (not shown). Above 0.6 T, the position of the line follows what is expected for an excitonic transition [large open triangles in Fig. 4(a)] in the presence of the giant Zeeman effect. This confirms that this transition corresponds to a positively charged exciton, with the excitation of an electron-hole pair involving an empty $|\frac{3}{2}\rangle$ heavy hole subband, in the presence of $|\frac{3}{2}\rangle$ heavy holes.

A less intense line can be noticed at higher energy in Fig. 3(b), at intermediate field (2 to 7 T). It shifts linearly with the field [small open triangles in Fig. 4(a)]. The distance between this line and the X^+ line in σ^- polarization is very close to the sum of cyclotron energies of the electron and the heavy hole (see below). Actually, this splitting is also very close to that measured in *n*-doped CdTe QW (Ref. 45) between the X^- line and a line shifting linearly with field, observed in σ^- polarization while the X^- line is seen in σ^+ polarization, and attributed to an “exciton-cyclotron resonance.” This exciton-cyclotron resonance implies the formation of an exciton and the promotion of an electron to the first excited Landau level, so that the shift is determined by the cyclotron energy of the electron (it is slightly larger due to a recoil effect). The same interpretation (exciton-cyclotron resonance) cannot be applied to our case, since the splitting for such a line in the presence of a hole gas should be close to the cyclotron energy of the heavy hole, which is definitely smaller. The origin of this line in our case is still unclear.

The σ^+ spectra are qualitatively different. The asymmetric absorption line decreases as the density of $|\frac{3}{2}\rangle$ holes increases, but the threshold can be followed up to about 3 T. Then sharper lines successively emerge, shift linearly to

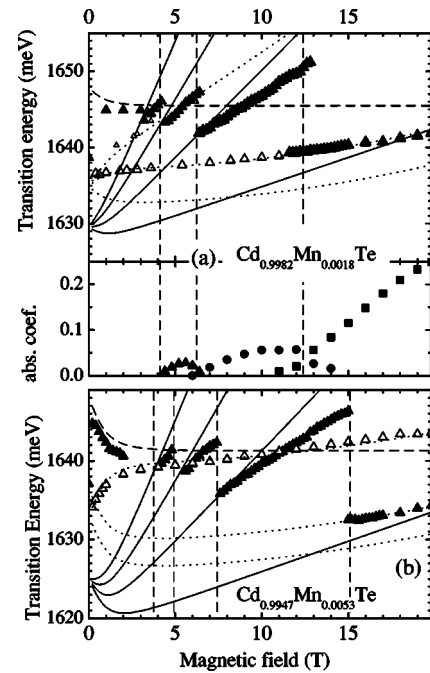


FIG. 4. Position of the absorption lines vs applied magnetic field. (a) $\text{Cd}_{0.9982}\text{Mn}_{0.0018}\text{Te}$ QW (sample N2); open symbols are for experimental data in σ^- polarization, full symbols for σ^+ polarization; dotted lines assume excitonic-like variations (normal and giant splitting and diamagnetic shift), with the zero-field energy as only adjustable parameter; solid lines assume Landau levels with the theoretical masses and the normal and giant Zeeman effects, with the zero-field energy as only adjustable parameter. The dotted line with a higher slope is shifted from the exciton in σ^- polarization by the Landau fan splitting (sum of cyclotron resonances). The dashed line shows the position expected for the absorption threshold at low field (it includes the normal and giant Zeeman effects and the Moss-Burstein shift added to the zero-field energy of the Landau fan, with no adjustable parameter). The lower part shows the intensity of each line in σ^+ polarization. The vertical dashed lines show the magnetic field values corresponding to integer filling factors. (b) same as (a), for sample N5, with a $\text{Cd}_{0.9947}\text{Mn}_{0.0053}\text{Te}$ QW.

higher energy [Fig. 4(a)], and vanish [see the intensity in the lower part of Fig. 4(a)]. Finally a single line progressively gains in intensity. We naturally ascribe this series of lines to the presence of the Fermi energy on successive Landau levels.

The description of Landau levels in the valence band is a complicated matter. In the simplest approximation the in-plane effective mass is $m_{hh} = m_0(\gamma_1 - 2\gamma_2)^{-1}$. Taking Luttinger parameters γ_i from Ref. 46, one obtains $m_{hh} = 0.17m_0$. Using a more complete model of the valence band, a slightly larger value, $m_{hh} = 0.25m_0$, was inferred.⁴⁷ This value will be used below, although it has not been confirmed experimentally. In addition, the transition energy is strongly affected by carrier-carrier interactions: staying with II-VI compounds, examples of such effects have been described in details for *n*-type CdTe and (Cd,Mn)Te QW's.⁴⁸ However, the degeneracy of the Landau levels remains unchanged and it is independent of material parameters. As only $|\frac{3}{2}\rangle$ holes are involved, so that each jump occurs from one Landau level to the next one with the same spin, we determine a filling factor $\nu = 1$ at *B*

=12.5 T, $\nu=2$ at $B=6.2$ T, and so on, as shown by vertical dashed lines in Fig. 4. The carrier density in this QW is thus determined to be $p=3.1 \times 10^{11} \text{ cm}^{-2}$.

Figure 4(a) shows as solid lines the field dependence expected for transitions between Landau levels, with an electron mass $m_e=0.11m_0$ and a transverse hole mass $m_{hh}=0.25m_0$, the normal Zeeman effect, and the giant Zeeman effect determined on the depleted QW. Using the zero-field energy as the only adjustable parameter, we obtain a relatively good agreement for the position of the lines when they emerge at $\nu=2$, $\nu=3$, and $\nu=4$. Once again, this is a crude approximation since it neglects the actual structure of the fan of Landau levels in the valence band (but the larger contribution is due to the conduction band) and carrier-carrier interactions (but these are minimal at integer filling factors). A precise description of these transitions is out of the scope of this paper.

We will show below that the zero-field energy of this Landau fan nearly matches the energy of a PL line, which appears to be close to the band to band recombination at $k=0$. The fact that this energy of a PL line at zero field is smaller than the excitonic transition energy is not surprising, since the PL band-to-band transition at $k=0$ leaves an excitation in the system: the exciton initial state is lower in energy, even if the transition energy is larger. This paradox does not appear in transmission: Figure 4(a) shows (dashed line) what is expected for the band-to-band transition at Fermi wave vector k_F ; it contains the normal and giant Zeeman effects and the kinetic energies of the electron and the hole both at k_F (so that it is drawn through the middle point between the two relevant branches of the Landau fan at each integer filling factor). We may note that it reasonably agrees with the position of the absorption line measured in the field range from 1 to 3 T.

Figure 4(b) displays the transition energies observed on sample N5, i.e., with a slightly larger Mn content; the carrier density is found to be $p=3.8 \times 10^{11} \text{ cm}^{-2}$. Both samples exhibit rather similar transmission spectra. We may notice that the transmission lines in the two polarizations at filling factor below unity are accidentally superimposed in sample N2 (a), but are clearly separated by the larger Zeeman splitting in sample N5 (b).

D. Hall effect

Hall effect and mobility measurements have been performed on several p -type doped CdTe and (Cd,Mn)Te quantum wells with a six-contact Hall structure. Gold Ohmic contacts to the buried QW's have been obtained by growing a heavily-nitrogen-doped ZnTe/(Cd,Zn,Mg)Te contact layer on top of the modulation-doped quantum well structures with a 20 nm spacer.³² Standard dc Hall effect and mobility measurements have been carried out in a helium flow cryostat from 300 K down to 15 K and with magnetic fields up to 1 T. The extremely high contact resistance below 15 K, due to freezing in the barriers, did not allow us to study the transport properties at lower temperatures. The integrated carrier density was deduced from the slope of the Hall resistance with respect to the magnetic field.

An example of carrier density as a function of the inverse of the temperature was given for four different samples in Ref. 32. A decrease of the measured carrier density observed between 300 and 100 K is attributed to the freezing of the residual holes in the barrier (holes that have not been transferred to the QW). Below 100 K and down to 15 K, a constant carrier density is observed and attributed to the conduction of the degenerate hole gas in the QW. In the four samples studied, the values of the 2D hole gas carrier density vary between $2.4 \times 10^{11} \text{ cm}^{-2}$ and $3.2 \times 10^{11} \text{ cm}^{-2}$, in agreement with the values deduced from optical spectroscopy (see discussion in Sec. V).

The Hall mobility increases almost linearly up to $1000 \text{ cm}^2/\text{Vs}$ with decreasing temperature from 300 K down to 15 K. This leads to a typical mean free path of the 2D hole gas of the order of 10 nm. This is a lower bound, however, since we observed a strong broadening of the PL spectra of the samples prepared for Hall studies, which had to be glued on the sample holder and appear to be highly strained.

IV. PHOTOLUMINESCENCE: BAND-TO-BAND VERSUS CHARGED EXCITON

This section is devoted to the description of the PL spectra and the effect of the Zeeman splitting: first, in Sec. IV A, we show the destabilization of the charged exciton—in favor of the neutral exciton—in a weakly doped QW. Then, in Sec. IV B, we show that a similar effect occurs in a QW with a larger carrier density. Finally, we describe more precisely the case of a partially polarized carrier gas in Sec. IV C.

A. Low concentration: charged and neutral excitons

We start the discussion of the PL spectra by the limit of low carrier density. Figure 5(a) shows PL spectra at different values of the magnetic field, in both circular polarizations, observed on sample N3 with 0.37% Mn in the QW (which allows us to follow the PL lines over the whole field range without overlap with the PL from the substrate). The carrier density was decreased by illumination with an Ar laser (which at the same time excites the PL) and can be estimated to be below $2 \times 10^{10} \text{ cm}^{-2}$ in the conditions of Fig. 5(a). The identification of the lines is based on the comparison between PL spectra and transmission spectra with white light [see Fig. 10(a) for the comparison done on another sample]. At zero field, the spectrum is dominated by a single line related to the charged exciton. A much weaker line due to the neutral exciton appears as a shoulder on the high-energy side. When applying the magnetic field, the relative intensity of both lines changes. In σ^- polarization, the neutral exciton line (the shoulder) disappears completely above 0.3 T, and the intensity of the charged exciton line progressively decreases; it disappears at 1 T. Figure 6(b) shows the intensity of each line. In σ^+ polarization, the PL intensity of the neutral exciton increases with respect to the X^+ one. The intensities of both lines become comparable at 0.6 T, and at higher fields the neutral exciton line dominates the spectra.

We have checked on samples with different Mn contents (not shown) that the transition from the charged to the neu-

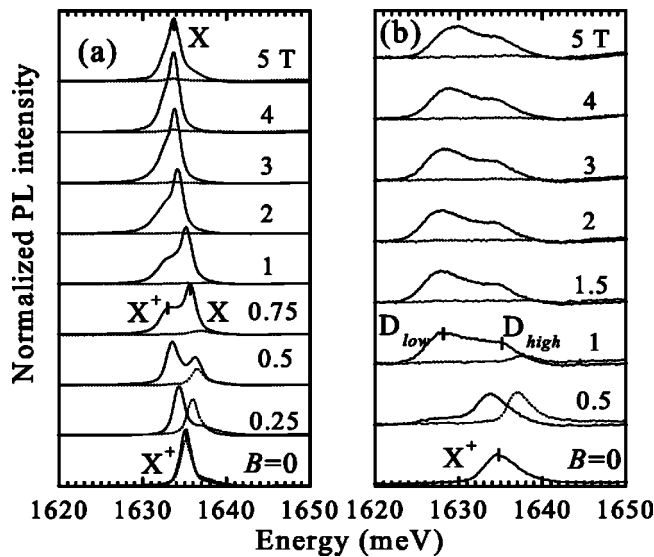


FIG. 5. (a) PL spectra, at 1.7 K, with various values of the applied field, from a Cd_{0.9963}Mn_{0.0037}Te QW (sample N3); the PL was excited using an Ar-ion laser, which almost completely depletes the QW. Solid lines are for σ^+ spectra and dotted line for σ^- ; (b) same as (a), but with excitation with a Ti-sapphire laser with photon energy below the barrier gap, which has no effect on the density of the carrier gas.

tral exciton is governed by the value of the giant Zeeman splitting. This destabilization of the charged exciton in favor of the neutral exciton can be understood as the result of the different Zeeman splittings of the three-particle system (two holes and an electron) either arranged as a charged exciton, or containing a neutral exciton. A schematic diagram of the three-particle levels is shown in Fig. 6(a). When applying a magnetic field the two states of the three-particle system experience different giant Zeeman shifts. In the fundamental state of the charged exciton, the two holes are arranged in a singlet state; therefore the Zeeman shift of the three-particle system is equal to the shift of the electron only, which is

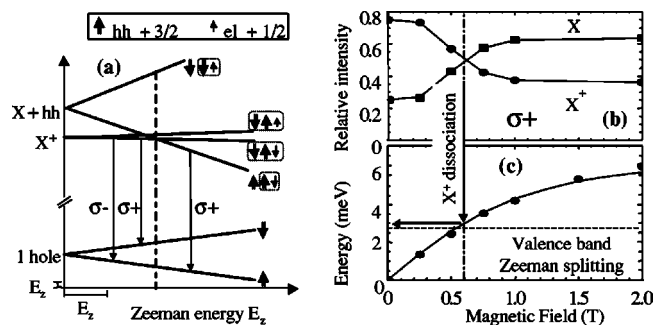


FIG. 6. (a) Three-carrier diagram of optical transitions. Single arrows show the electron spin and double arrows the hole spin; the dash-dotted line marks the level crossing. (b) Relative intensities of the X and X^+ photoluminescence lines measured in σ^+ polarization for sample N3, Cd_{0.9963}Mn_{0.0037}Te QW, under illumination by an Ar-ion laser. (c) Comparison of the valence band Zeeman splitting (points and solid line) and the X/X^+ splitting (dashed horizontal line) for sample N3. Dot-dashed vertical lines mark the field at which the X/X^+ crossing occurs.

rather small: in (Cd,Mn)Te, the giant Zeeman shift of the heavy hole is four times larger than the electron shift. The bright state of the neutral exciton is composed of a hole and an electron with opposite spin directions, and the remaining hole is free; therefore the component with its two holes in the majority band (which emits in σ^+ polarization) shows a strong redshift under applied field, equal to the sum of the individual shifts of the electron and the two holes. At zero field, the charged exciton state is lower in energy since it is a bound state, and this remains true at low field. When the heavy-hole Zeeman splitting is equal to the X^+ dissociation energy [Figs. 6(a) and 6(c)], the neutral exciton level crosses the level of the charged exciton emitting in the σ^+ polarization, so that the neutral exciton level becomes lower in energy. The mechanism is similar to the crossing induced by the giant Zeeman splitting between the A^0X bound excitons and free excitons in bulk diluted magnetic semiconductors.⁴⁹

The ratio of the X and X^+ intensities experimentally observed [Fig. 6(b)] varies smoothly, making it difficult to precisely point out the crossing, which is expected when the value of Zeeman splitting equals the binding energy of the trion [Fig. 6(c)]. Actually, the intensity ratio results from the dynamics between the X and X^+ states, and, in addition, disorder introduces a broadening of the densities of states. It was already recognized¹¹ that the dynamical nonequilibrium distribution between the X and X^+ populations leads to the observation of some PL intensity from the upper level. In particular, at zero field, the neutral exciton luminescence is observed due to a formation time of the charged exciton comparable with the decay time of the neutral exciton. This formation time is strongly sensitive to the carrier density:⁵⁰ As the carrier density is increased, it becomes shorter so that a more abrupt transition is expected.

The main result of this section is that the giant Zeeman splitting of the hole can be large enough to destabilize the singlet state of the charged exciton, in favor of the σ^+ emitting neutral exciton, which is such that the two holes have parallel spins.

B. Photoluminescence in the presence of a 2D hole gas

The main features of the PL spectra at moderate Zeeman splitting have been described in Ref. 23. It was shown that, in σ^- polarization, the PL line and the absorption line coincide (but for a constant Stokes shift smaller than 1 meV) over a well defined range of the applied field where the hole gas is fully polarized, an example is given by the σ^- spectra (dashed line) in Fig. 10(c). It was shown also that in the same field range the PL line in σ^+ polarization is shifted by the excitonic Zeeman splitting. This suggests that both lines are due to the charged exciton. We will come back to this point—and to the shift that appears between the absorption and PL lines at smaller field—in Sec. IV C. First we keep in mind this assignment of the PL lines at low Zeeman splitting to the charged exciton and we wish to introduce a new feature that appears at larger Zeeman splitting.

1. Appearance of a double line at large Zeeman splitting

Figure 5(b) shows PL spectra, at different values of the applied magnetic field, in both circular polarizations ob-

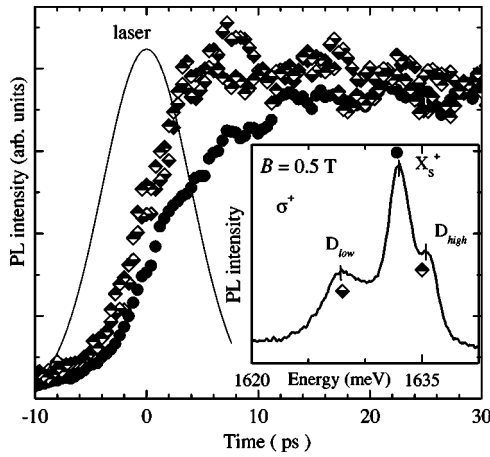


FIG. 7. Time-resolved photoluminescence of sample N4 ($\text{Cd}_{0.996}\text{Mn}_{0.004}\text{Te}$ QW) measured in σ^+ polarization in a magnetic field of 0.5 T close to the crossing of the excited levels. Symbols give the temporal profiles after excitation by the laser pulse (solid line), detected at different energies corresponding to different components of the PL (marked D_{low} , X_s^+ , D_{high} on the spectrum in the inset).

served on the same sample N3 as discussed before but measured with Ti-sapphire laser excitation, hence without above-barrier illumination. The carrier density will be estimated as explained below as $p = 4.2 \times 10^{11} \text{ cm}^{-2}$. Similarly to the lower-density case, a single line is observed at zero field. At low field (see the spectra at 0.5 T), the giant Zeeman effect is sizable; the high-energy line is polarized σ^- and reasonably sharp, while the low-energy line, polarized σ^+ , is broader, with a weak tail on the low-energy side. We continue to assign this PL to the charged exciton,²³ and we will come back to this later. At higher field, the PL is fully polarized σ^+ , with a typical double structure containing a high-energy line labeled D_{high} in the following, and a low-energy line labeled D_{low} . The transition from the single to the double line in σ^+ polarization occurs at about 0.6 T, close to the value causing the X/X^+ crossing at low carrier density. The shape of the double line remains constant up to 3 T in Fig. 5(b). Above this field a progressive change of shape occurs, which we attribute to the emergence of the Landau levels as seen in Fig. 4.

We will discuss this evolution in the same spirit as the one observed from charged to neutral excitons for low carrier density. More precisely, we will show that the double line involves a unique initial state, which crosses the charged exciton state when the Zeeman splitting exceeds some value.

First, the character of the optical transition involved in this double line was examined by time-resolved spectroscopy. The inset in Fig. 7 shows a time-integrated spectrum taken in σ^+ polarization in a field of 0.5 T. This is the field range for which both the single and the double lines are observed, and the hole gas is already fully polarized. PL was excited with a ps pulse also with σ^+ polarization. The decay time of all three lines was found to be the same, about 100 ps. Rise times, however, were quite different. PL traces related to the double line (traces D_{high} and D_{low} in Fig. 7) exhibit a rise time faster than 2 ps and limited by the reso-

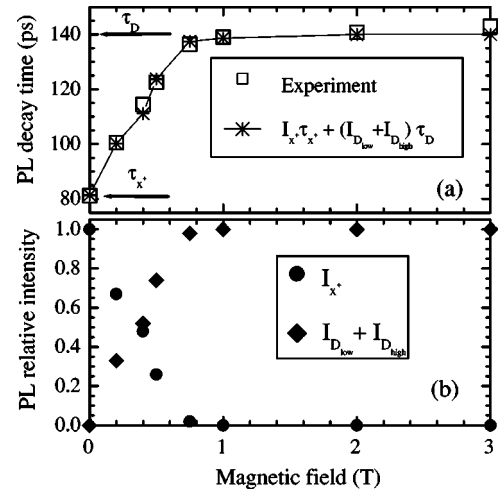


FIG. 8. Sample N4, $\text{Cd}_{0.996}\text{Mn}_{0.004}\text{Te}$ QW (a) integrated PL decay time measured in σ^+ polarization, as a function of the magnetic field; open squares denote the experimental values, stars represent the average of two times: $\tau_{X^+} = 80$ ps and $\tau_{D_{low}} = \tau_{D_{high}} = 140$ ps (arrows), weighted by the intensities of each of the two components of the PL spectra, plotted in (b). (b) Relative time-integrated intensities of the two components of photoluminescence spectra: double line D_{low}/D_{high} (squares), and excitonic line (circles) measured in σ^+ polarization, as a function of the magnetic field.

lution of the set up. A significantly larger rise time, larger than 3 ps, is measured on the single line (trace X_s^+ in Fig. 7). When increasing the magnetic field the rise times of both components of the double line remain the same and very fast. This we use as a first argument that the two components D_{high} and D_{low} of the double line involve an initial state, which is different from the initial state of the single line observed at lower field.

The values of the rise times also support the assignation of the single line to a state involving a two-hole singlet and the double line involving an initial state where all holes have the same orientation as in the ground state. The σ^+ -polarized light creates an electron-hole pair where the hole has the same spin orientation as those of the carrier gas (majority spin). Hence the charged exciton luminescence involves a heavy-hole spin flip in order to form the singlet hole pair. In fact the time of 3 ps compares well to the heavy-hole spin flip time observed in X^- states.^{17,51} On the other hand, the fast rise of the double line suggests that no spin flip—and hence no singlet hole pair—is involved in this double line.

The picture of a crossing of initial states is further supported by the variation of the decay time versus magnetic field. Figure 8(a) presents the dependence of the integrated PL decay time versus magnetic field. This time increases by almost a factor of 2 when increasing the magnetic field from 0 to 1 T, which coincides with the transition from the single PL line to the double line. The observed decay time coincides exactly with the average of the decay times at 0 T and 3 T, weighted by the relative intensities of the two PL components, presented in Fig. 8(b). Such a behavior is predicted by a rate equation model if there are only two field-independent channels for radiative decay, related to the two PL mechanisms giving rise to the single and double lines,

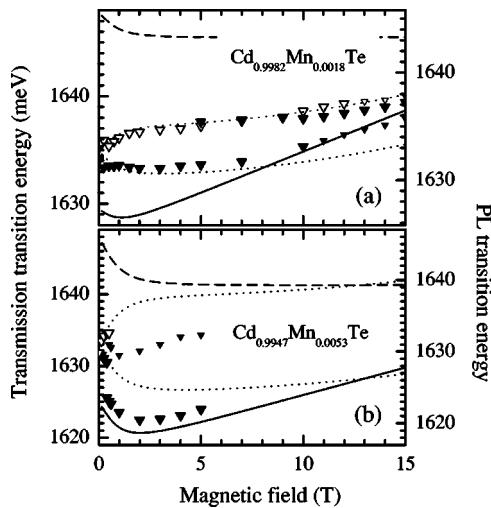


FIG. 9. Comparison of the transition energy in PL (down triangles) vs transmission (lines showing the fits used in Fig. 4). Note that the PL and transmission scales have been shifted (see text). (a) Sample N2, $\text{Cd}_{0.9982}\text{Mn}_{0.0018}\text{Te}$ QW and (b) sample N5, $\text{Cd}_{0.9947}\text{Mn}_{0.0053}\text{Te}$ QW, as in Fig. 4.

respectively. The double line is associated with a decay channel (140 ps) slower than that of the charged exciton line (80 ps), suggesting a weaker correlation.

We conclude that the transition between the two kinds of PL spectra (excitonic or double line) is related to the level crossing of the initial states, with one state involving a pair of holes forming a singlet (charged exciton recombination at low field), the other one with all hole spins having the same orientation. Here again, the field at which the transition takes place is defined by a value of the valence band Zeeman splitting (see below the compilation over various samples), and the transition will be more or less abrupt, depending on the relaxation processes between the two levels. It is worth mentioning that, as expected, the transition is more abrupt in the cw experiment with very weak excitation than in the time-resolved experiment for which the system is excited farther from quasiequilibrium conditions.

Now we come back to the analysis of the energies of the PL lines in sample N5, for field values such that the hole gas is fully polarized (above 0.2 T in this sample, see below). Figure 9(b) compares the positions of the transmission lines [the fits from Fig. 4(b)] to the positions of the PL lines in the same sample. Transmission spectra were measured in one run at the Grenoble High Field Laboratory while we used a Ti-sapphire laser to excite the PL in a different run: to take into account the expected Stokes shift (usually at most 1 meV when transmission and PL were measured in the same run) and also to allow for a possible fluctuation of sample characteristics between the regions of the sample observed during the two runs, the PL scale was shifted (by 2 meV), so that PL and transmission lines in σ^- polarization were made to coincide at one field where both are observed. As shown previously²³ for sample N2, and below in Fig. 10 and Fig. 11(a) for sample N4, this plot confirms that the PL transition in σ^- polarization closely matches the position of the charged exciton measured in transmission over a finite

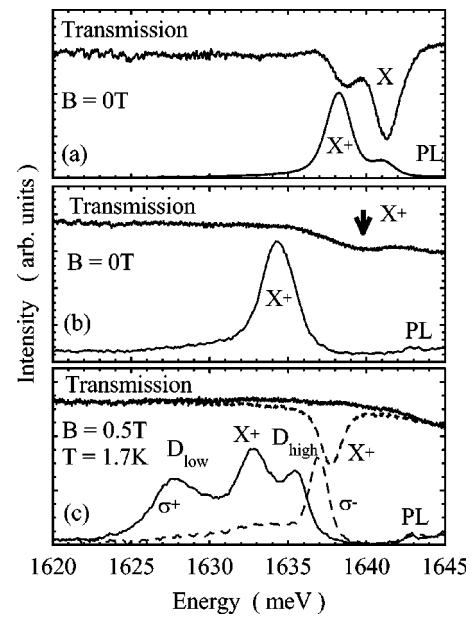


FIG. 10. Example of the transmission and PL spectra at zero magnetic field (a and b) and magnetic field 0.5 T (c) for sample N4, ($\text{Cd}_{0.996}\text{Mn}_{0.004}\text{Te}$ QW). In (a) the sample was illuminated by a strong blue light, which almost completely depleted the QW. In (b) and (c) there was no above barrier illumination so there was an equilibrium density of carriers. Solid lines are for σ^+ spectra and dashed lines for σ^- . The data from (b) and (c) were used to draw Fig. 11.

field range, but that appears to be true also for the σ^+ PL at low field (below 0.3 T in this sample). Above this field value, the low-energy component of the PL double line (D_{low}) is close to the position expected for the band-to-band transition (lower branch of the Landau fan). The high-energy component of the σ^+ doublet (D_{high}) is marked with smaller symbols because its intensity is small in this sample (in addition at this particular Mn content it overlaps with the substrate PL so that its energy was determined with less accuracy). Note also that the difference in radiative decay times observed on sample N4 in Fig. 8(a) (80 ps and 140 ps, respectively) is consistent with such an excitonic character of the single dichroic line at low field versus a band-to-band character of the double line $D_{low}-D_{high}$. The excitonic decay time is expected to be significantly shorter than the one measured in the band-to-band transition, which implies a weaker electron-hole correlation.

The jump to the double line is induced by the giant Zeeman splitting. This was checked on all samples with a Mn content between 0.2% and 1%. For example, in sample N2 of Fig. 4(a), with the lowest Mn content of our series, the jump is not observed [Fig. 9(a)] up to 10 T, although the hole gas is fully polarized already at 0.6 T. A progressive change in the slope of the σ^+ PL energy versus field would agree with the same change of nature of the PL transition, from excitonic to band-to-band, but Landau levels cannot be ignored at such high fields. In this sample with a very low Mn content the maximum Zeeman splitting is large enough to fully polarize the hole gas, but too small to destabilize the charged exciton singlet state.

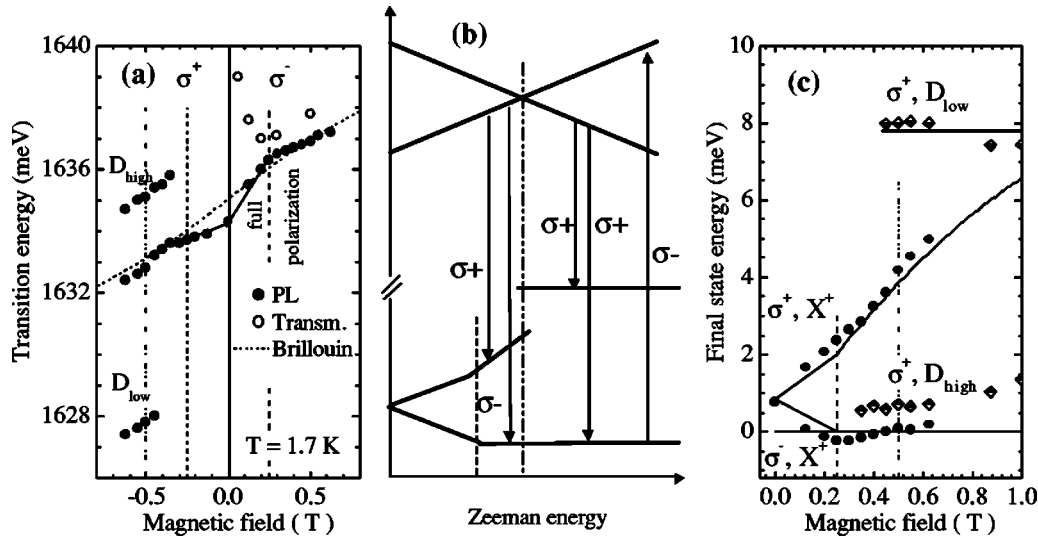


FIG. 11. (a) Positions of the transmission lines (open circles) and PL lines (full circles) vs the applied magnetic field, in the low-field range, for sample N4, $\text{Cd}_{0.996}\text{Mn}_{0.004}\text{Te}$ QW. The σ^- data are plotted at negative fields. The dotted line gives the Brillouin function determined at high field. (b) Schematic diagram of the initial and final states and of the optical transitions. (c) Experimentally determined energies (see text) of the final states of optical transitions, obtained from data in (a); diamonds are for the double line (D_{low}, D_{high}), circles for the excitonic line, and the solid lines are drawn using the energies of initial and final state plotted in (b). In all 3 panels, dashed vertical lines indicate the field values for complete hole polarization, and the dash-dotted vertical line indicates the destabilization of X^+ .

Let us briefly summarize our findings at this point. In the presence of a fully polarized hole gas with a density of several 10^{11} cm^{-2} , PL spectra exhibit a crossing of the excited states that behaves quite similarly to the X/X^+ crossing observed at low hole density. At fields below the crossing, we observe a single PL line in both σ^+ and σ^- polarizations. Its position coincides with the charged exciton X^+ (which is observed to emerge in σ^- transmission from the charged exciton when the carrier density increases) and it has a short decay time (as expected for an exciton) and a long formation time (as expected for the singlet configuration of the two holes in the charged exciton). Thus, the initial state of this transition is likely to be linked to the charged exciton state well identified at low carrier density. Above the crossing, the giant Zeeman energy due to the two-hole singlet is too large. The excited state, which is now lower in energy, gives rise to a double PL line, $D_{low}-D_{high}$; it does not contain a two-hole singlet, so that its formation time is shorter, and the electron-hole correlation is weaker so that the lifetime is longer. Finally, the position of the low-energy component D_{low} is close to what we would expect for a band-to-band transition at $k=0$. Some characteristic spectra are given in Fig. 10 for one sample, in PL and transmission.

The crossing of singlet and triplet levels plays also an important role in the polarization of the total PL signal. The two-hole singlet states, which are the initial states of PL transitions in both circular polarizations, differ only by the spin of the electron. Thus the splitting of this level is only $1/5$ of the exciton Zeeman splitting. Such a small splitting leads to comparable occupations of both states and hence to comparable PL intensities in both polarizations. Additionally, the spin flip time of the electron is relatively long and even comparable to the X^+ lifetime.^{11,50} This prevents fast spin relaxation between the charged exciton singlet states. A com-

pletely different situation takes place after the singlet-triplet crossing. Then only the σ^+ transition is possible from the lowest initial state. The opposite triplet state has an energy higher by twice the value of the exciton splitting. This is in agreement with the PL polarization experimentally observed: The σ^- line intensity remains almost the same as that in σ^+ below the jump, and it vanishes completely after the jump.

The conclusion of this section is that the giant Zeeman effect induces a crossing between an excited state that involves a two-hole singlet and another one where all holes are in the majority spin subband. There are strong hints that the first state is the singlet state of the charged exciton X^+ ; the second one could be an uncorrelated electron-hole pair (initial state of band-to-band transitions) or a weakly correlated “triplet state.” With these attributions in mind, we will continue the analysis of the spectra.

2. Final states in PL transitions

We now discuss the final states assuming the same field dependence of the initial states as in the low-density case (dependence determined by the spin singlet or spin triplet configuration of the two holes). We will show that each of these initial states gives rise to two transitions: one toward the ground state, and another one leaving the hole gas in an excited state. In order to describe the PL in the case of a large density of the hole gas, we redraw the three-particle scheme introduced to describe X and X^+ [Fig. 6(a)], now measuring all energies with respect to the ground state of the hole gas [Figs. 11(b) and 12].

The simplest transition takes place in σ^- polarization at sufficiently high magnetic field, so that the hole gas is fully polarized. For each field, below the destabilization of the singlet state where σ^- PL disappears, both the PL and absorption exhibit a single σ^- sharp line, at almost the same

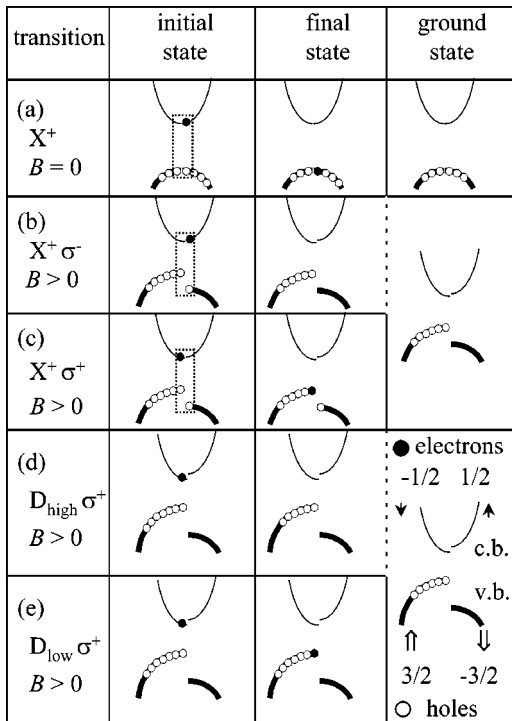


FIG. 12. Schematic diagram of the initial and final states in optical transitions from Fig. 11.

energy (but for a small, constant, Stokes shift). Therefore we attribute this line to the transitions between the ground state of the carrier gas and some exciton complex. Due to the selection rules in transmission this complex is identified as a charged exciton with a two-hole spin singlet and a $+1/2$ electron. In σ^- PL, the $+1/2$ electron recombines with the minority (upper energy) $-3/2$ hole of the singlet, leaving all the holes in the lower, majority spin subband. The final state is the ground state, Fig. 12(b). In σ^+ polarization, the absorption transition involving the singlet charged exciton state is forbidden. However, if the electron spin flips to $-1/2$, the PL transition is allowed in σ^+ polarization, but does not lead to the ground state of the hole gas: The $-1/2$ electron recombines with a $+3/2$ hole, leaving one $-3/2$ hole in the opposite subband. Therefore the final state is an excited state of energy equal at least to the hole Zeeman splitting [Fig. 12(c)].

When the two excited states cross each other, the initial state of the transition changes its character. Experimentally, a PL jump is observed in σ^+ polarization, where the single PL line turns to a double one. We now identify the final states of the transitions related to the double line by considering the crossing. At this particular field, the initial states in σ^+ polarization are degenerate, and the only difference between the two singlet initial states in σ^+ and σ^- polarization is the Zeeman splitting of the electron. We already know that the final state in σ^- is the ground state of the hole gas. According to our measurements for all samples, at the crossing, the upper component of the PL double line, D_{high} , has almost the same energy as the σ^- transition [see Fig. 13(a)]: the difference, around 1 meV, is partly due to the electron Zeeman energy (of the order of 0.5 meV at the jump), and what remains might be due to the different shapes of the two lines.

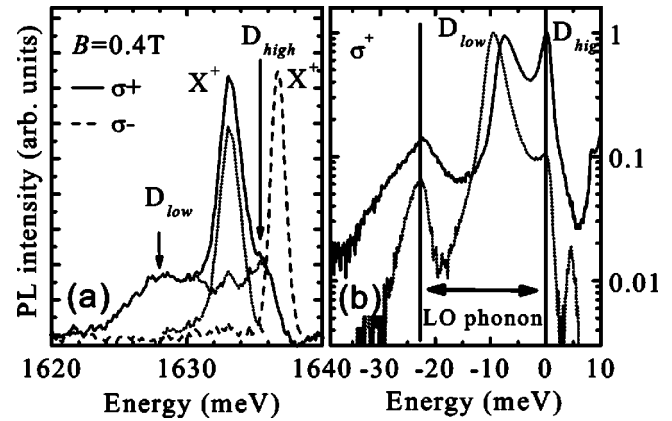


FIG. 13. (a) cw PL spectra of sample N4 at level crossing (linear scale); the solid line gives the experimental PL spectrum in σ^+ polarization and the dashed line the experimental spectrum in σ^- polarization; the dotted lines give the proposed decomposition of the σ^+ line into the double line (D_{high} - D_{low}) and the excitonic one. (b) Typical spectra in σ^+ polarization for samples N4 (at 1 T, solid line), and S7 (QW doped from surface states, at 0.5 T, dotted line); the energy scale is with respect to the position of the upper component of the PL double line, D_{high} , and the intensity scale is a log scale.

Therefore the final state of D_{high} is also the ground state of the heavy-hole gas [Fig. 12(d)], while D_{low} leaves it in an excited state [Fig. 12(e)].

Note that in a band-to-band description of this double line, the transition D_{low} is a direct one involving an electron and a hole both at $K=0$ (thus leaving the hole gas in an excited state of energy equal to the Fermi energy of the spin-polarized gas, $2E_F$, keeping the notation E_F for the Fermi energy at zero field), while D_{high} is an indirect one where the electron recombines with a hole at Fermi level, leaving the hole gas in the ground state. This indirect transition might be allowed due to disorder or many body effects. In fact we observe that the relative intensity of this line D_{high} with respect to D_{low} varies from sample to sample. The indirect character is further supported by the observation of the LO-phonon replica: In the magnetic field in σ^+ polarization, a clear phonon replica is observed only for D_{high} [Fig. 13(b)]. This is characteristic for transitions that are indirect in k space, so that the replica includes the phonon wave vector in the conservation rule.

From a purely experimental point of view, the splitting of the double line gives the energy of the excited state of the hole gas towards which the transition takes place in the case of the lower component. The variation of this energy versus carrier concentration will be discussed later in Sec. V B.

The ordering of the transition energies may be different from the ordering of the initial states involved in the transition: the difference is due to the energy of the final state, which of course is not necessarily the ground state. Hence, an excitonic transition may appear at an energy higher than a band-to-band transition. This is the case here if we compare the charged-exciton line in σ^- polarization (which has the ground state as the final state) and the intense low-energy component of the double line, which leaves the hole gas in an excited state.

Note also that the hole Zeeman splitting, for the destabilization field (the field at which the level crossing takes place), is a measure of the binding energy of the singlet state at zero field. We found this energy to lie between 2 meV and 3 meV for all measured samples, independently of the carrier density (Fig. 15).

Summarizing this part, the PL has an excitonic character for σ^- polarization, and in σ^+ at low field. At high field in σ^+ polarization, a double line is observed. This change is due to a level crossing between the charged-exciton state that contains two holes in a singlet configuration, and an initial state of the double line where all holes are in the majority spin subband: due to the strong Zeeman energy, the hole pair involved in the charged exciton flips from the singlet configuration to a triplet. Several characteristics of this double line (including its shape, but also the dynamics and the coincidence in energy of the lower component with the energy between first Landau levels extrapolated to $B=0$) suggest that this transition is quite similar to a band-to-band transition. The upper component of the double line involves the transition to the fundamental state of the hole gas. In a band-to-band picture, such a transition is an indirect one since the electron recombines with a hole at Fermi level. The lower component of the double line is related to a transition towards an excited state of the hole gas. This excitation involves no spin flip (all holes are in the majority spin subband). In a band-to-band picture, it is the state after recombination at $k=0$, in which one electron is left at the top of valence band. Deviation from the band-to-band picture, showing that some correlation exists in the electron hole pair, will be described in Sec. V B.

C. Low fields: Incomplete hole gas polarization

For low magnetic fields, the dependence of the PL energy on magnetic field significantly deviates from the curve describing the giant Zeeman effect in (Cd,Mn)Te. An example is given in Fig. 11(a) for sample N4. The transition energy measured at zero field is 1 meV below the Zeeman curve [dotted line in Fig. 11(a)]. This difference decreases for both polarizations when increasing the magnetic field, and vanishes for a field stronger than a certain value, equal to 0.2 T in sample N4. Above this field, the PL line in σ^- polarization coincides with the absorption line (but for a small constant Stokes shift). This lets us conclude that this point is a point of complete polarization of the hole gas.

This can be used to obtain an information on the final state involved in the transition. This is done by assuming, as above, that the energy of the initial state (the charged exciton) involves only the electron Zeeman shift, so that the energy of the final state [Fig. 11(c)] is deduced from the transition energy. As expected, in σ^- polarization, the final state is the ground state of hole gas. In σ^+ polarization, the same transition leads to an excited state of the hole gas, with one hole transferred from the majority spin subband of the valence band, to the empty spin subband. This excited state is a spin excitation of the hole gas. The k selection rule is obeyed if this excitation is a spin wave at $k=0$ or, in an independent-carrier description, there is one electron at $k=0$ in the major-

ity spin subband and a hole at $k=0$ in the empty spin subband: the excitation energy is equal to the Zeeman splitting of the valence band, $2E_Z$ where E_Z is the Zeeman shift, as experimentally found [Fig. 11(c), above 0.2 T].

Similarly, we can calculate the energies of the final state also for the incompletely polarized hole gas. We still assume that the electron is left at the top of the valence band. Then the energy of the final states are E_F+E_Z for σ^+ polarization and E_F-E_Z for σ^- polarization, where E_F is the Fermi energy of the hole gas measured from the top of the valence band at zero field. These energies are plotted schematically in Fig. 11(b), and compared to the experimental values below 0.2 T in Fig. 11(c). Figure 11(c) shows also that, as described in Sec. IV B 2, the final states of the double line are, to a good approximation, the ground state and an excited state of field-independent energy.

It is interesting to note that according to the proposed level diagram, the distance from the charged-exciton line to the upper component of the double line in σ^+ polarization is equal to the binding energy of the singlet. Thus, this binding energy (which was deduced above as being equal to the Zeeman splitting at the field where the jump occurs) can be measured directly on the spectra at the jump, as the splitting between two lines.

V. CHARACTERISTIC ENERGY SCALES OF THE SYSTEM

This section is devoted to discussion of characteristic energies related to the carrier gas. First, in Sec. V A, we compare different methods of determination of the carrier density. Then in Sec. V B, we discuss the energies of excitations of the carrier gas, the Zeeman energy necessary to completely polarize the hole gas, and its Fermi energy. Finally, in Sec. V C, we describe the evolution of the charged-exciton dissociation energy with carrier density.

A. Spectroscopic determination of the carrier density

In this section we wish to complete our set of methods of characterizing the hole gas in a QW. The carrier density is often determined from the shift between the PL and PLE or absorption lines: this is the so-called Moss-Burstein shift, which in the case of band-to-band transitions is the sum of the kinetic energies of holes and electrons at k_F . To increase the accuracy, these measurements can be carried out in a magnetic field, in which the hole gas is completely spin polarized, so that the magnitude of the shift is doubled. Here we profit from the samples for which the carrier concentration was determined by direct techniques, Hall effect in one sample and filling factors at high field in two samples. These three samples were also characterized by standard magneto-optics, and the so-called Moss-Burstein shift was obtained.

First we compare the values of the density obtained from filling factors of Landau levels in transmission and from Hall measurements, to the shift between the lower component of the double line in PL, D_{low} , and the absorption in σ^+ polarization [Fig. 14(a)]. The slope is very close to the value expected for the Moss-Burstein shift E_{MB} in a single-particle approach,

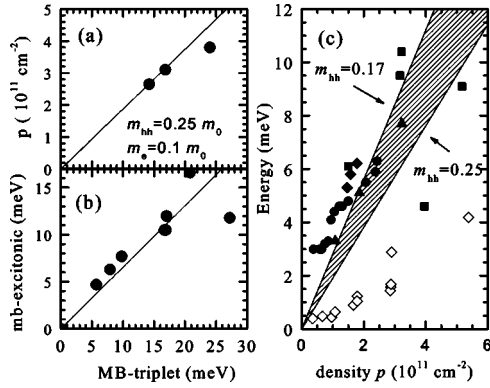


FIG. 14. (a) The hole gas density determined from filling factors in the Landau fan, or from Hall resistance, versus the polarized Moss-Burstein shift between the absorption line and the lower component of the double PL line, D_{low} , in σ^+ polarization; the solid line is the calculated slope using the electron and hole masses as described in the text. (b) “Excitonic mb shift” (measured in σ^+ polarization between the absorption line and the excitonic PL line, at a field such that the hole gas is completely polarized, but which is lower than the value where the level crossing occurs. The solid line is a linear fit. (c) Full symbols represent the splitting of the double line D_{high} - D_{low} —the energy of the final state involved in the D_{high} component—vs the carrier density. Note that two samples have been measured at different carrier densities, changed either optically (sample N4, triangles) or through an electrostatic gate (sample D3, circles and sample D50, diamonds). Open diamonds represent the valence band Zeeman splitting at complete hole gas polarization; gray area is the Fermi energy of the polarized hole gas.

$$p = \frac{m_0}{2\pi\hbar^2} \frac{m_e m_{hh}}{m_e + m_{hh}} E_{MB}.$$

This confirms that the double line is very close to a band-to-band transition. Therefore this is in principle the better choice for a spectroscopic determination of the carrier density.

However, the shift between the charged-exciton PL and the absorption line, at intermediate field, is usually much easier to measure. Here again, it can be measured in a magnetic field high enough to fully polarize the hole gas, but below the jump to the double line.²³ We will call this shift “the excitonic mb shift.” We find it to be a linear function of the real Moss-Burstein shift and of the carrier density [Fig. 14(b)]. In the present case this “excitonic Moss-Burstein shift” is smaller than the calculated Moss-Burstein shift by a factor of 1.5. Hence we confirm that this procedure²³ provides an accurate evaluation of the relative hole density, and even of its absolute value once a proper calibration has been done.

The final state in the σ^+ absorption process has to be discussed, probably by considering an excitation of the hole gas in the presence of the bound state (singlet trion). The intensity of this line rapidly decreases in σ^+ polarization, since it needs the presence of a minority spin hole to form the two-hole singlet state. Note that, for this reason, a clear distinction has to be made between the excitonic transition, observed in the presence of the incompletely polarized hole

gas, and the band-to-band transition, which does not include a singlet state and is observed (see Fig. 4) at field values up to a few teslas. However, the intensity of the two absorption lines, the charged-exciton transition in σ^+ polarization and the band-to-band transition, is too low, in a single QW sample, to allow a detailed study.

To sum up, we have several well-justified determinations of the carrier density (filling factors, Hall effect, MB shift between D_{low} and transmission), but the most convenient one is to measure the “excitonic mb shift” between the charged-exciton luminescence and the transmission line. This can be done at zero field, or, with a better accuracy, at moderate field; a preliminary calibration is needed (Fig. 14). It implies that the carrier densities quoted in our previous studies²³ were underestimated by a factor of 1.5.

One could think that the Zeeman effect needed to fully polarize the hole gas could be another way of determining its density. We will show below that this involves a strong contribution from carrier-carrier interactions.

B. Energy scales in the hole gas

As discussed above, the analysis of the PL in magnetic field allowed us to determine different characteristic energies of the completely or partially polarized hole gas. First of all, the reliable determination of the hole density allows us to calculate the Fermi energy at zero field in the single-particle approach:

$$E_F = \frac{\pi\hbar^2 p}{m_{hh}}.$$

In the fully polarized gas, it is $2E_F$. As mentioned in Sec. III, depending on the description of the valence band, the heavy-hole effective mass might vary from $0.17m_0$ up to $0.25m_0$. The range of possible values of the Fermi energy is marked by the gray area in Fig. 14(c).

The splitting of the double line (D_{high} - D_{low}) gives the energy of the excited state of the hole gas, which is the final state in the transition related to the lower component D_{low} . This excitation involves no spin flip, i.e., all carriers are in the majority spin subband. This energy increases with the carrier density, as shown in Fig. 14(c). In a single-particle band-to-band description, an electron at $k=0$ may recombine with any hole with wave vector between $k=0$ and $k=k_F$, particularly if the rule of conservation of the wave vector in the optical transition is relaxed by disorder. In a nonpolarized gas, the intensity is enhanced at the low-energy edge due to a larger recombination rate, and at the high-energy edge due to the so-called Fermi edge singularity. Then the width of the line is equal to the Fermi energy of the hole gas. One could imagine to have similar effects in a polarized gas (with a width equal to $2E_F$ for a fully polarized gas).

It is clear in Fig. 14(c) that at low carrier density the splitting of the double line is larger than the Fermi energy of the hole gas, and it appears to deviate from linearity. Recombination of electrons with a finite wave vector (due to slow relaxation) would add to that the kinetic energy of electrons up to k_F . This is, however, unlikely since the double line appears as a whole at the crossing, with a uniform lifetime

measured in time-resolved PL. This suggests that the initial state is unique, one possibility being the triplet state of the exciton, which is thought to have in some cases a small but finite binding energy with respect to the free carrier continuum. The energy in the final state should be discussed in terms of excitations of the hole gas (plasmon, combination of single particle excitations, many body excitations, etc.⁵²) with a total wave vector equal to k_F . At large carrier density, the $D_{high}-D_{low}$ splitting tends to match the Fermi energy, as expected for simple band-to-band transitions.

It is thus difficult to obtain the precise nature of the initial state of the double line, but for the fact that it involves holes sitting all on the majority spin subband. At very low carrier density, we have shown that the neutral exciton is most probably involved. It is not clear whether a triplet state of the charged exciton could be stabilized by the Zeeman energy. Up to now, triplet states have been described in nonmagnetic QW's at field values large enough to alter the orbital motion of the carriers,^{18–20,30,31} which is not the case here. At large carrier densities, these bound states will become more and more difficult to distinguish from an uncorrelated electron-hole pair, but for the fact that in the absence of interactions, the high-energy component D_{high} should vanish. We have found that the relative intensity of the two components of the double line changes from sample to sample. In the case of a band-to-band transition in the presence of a nonpolarized gas, the high-energy component is expected to be enhanced by disorder and by the formation of the Fermi edge singularity at low carrier density (which eventually evolves into the charged-exciton transition). The situation is different in the present case of a polarized gas. We clearly and systematically observe that the intensity of this high-energy component increases when the carrier density is decreased in one sample (by barrier illumination or by using a $p-i-n$ structure). But the intense line that subsists alone at very small carrier density is not the singlet state of the charged exciton, but the neutral exciton (or possibly a triplet state of the charged exciton, as discussed above).

We have no indication of a relationship with disorder (which could be induced by alloy fluctuations at larger Mn content or by the electrostatic disorder known to be present in the $p-i-n$ samples). In such disordered samples, we generally find that the charged exciton persists at larger values of the spin splitting. This might be an indication that in those samples, disorder more severely affects the bound states, likely to be easier to localize. This is in particular the case of samples with a larger Mn content, which display carrier-induced ferromagnetic interaction.⁵⁷ In such samples, we have indeed observed the jump from the charged-exciton PL to the double line: it could be induced not only by the giant Zeeman splitting under applied magnetic field, as in the present study, but also by the splitting due to the spontaneous magnetization.

Another characteristic energy is the valence band Zeeman splitting for which the hole gas is completely polarized. It is determined by the analysis of the evolution of the position of the PL and absorption lines. At this particular field, and in a single-particle approach, the Zeeman splitting of the valence band is equal to the Fermi energy. The comparison between the Zeeman splitting [which is well known in (Cd,Mn)Te]

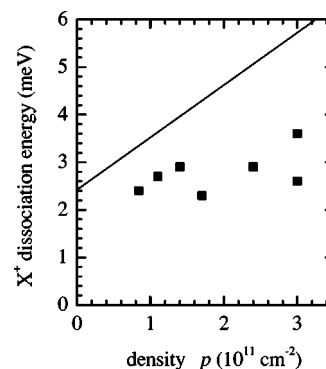


FIG. 15. Dissociation energy of the charged exciton, determined from the level crossing (squares) vs the carrier density; the solid line shows the $X-X^+$ splitting determined from absorption spectra in Ref. 23.

and the Fermi energy is given in Fig. 14(c). We find that the single-particle Fermi energy is over two times larger than the valence band splitting at complete polarization. Such an enhancement of the susceptibility of a carrier gas is known to be the result of many-body interactions.^{53–56} It is usually calculated for an electron gas. Our system gives a very unique and direct insight to those effects in a hole gas.

With this in mind, it is worth to come back to the discussion of the final state involved in the σ^+ transition with the charged exciton. This state was described in terms of single-particle excitations in Sec. IV C. However, one should note that this description holds only if one applies to the energy of these excitations the same reduction factor as for the Zeeman splitting needed to get full polarization (i.e., the inverse of the enhancement of spin susceptibility).

C. Spectroscopy and energies related to the charged exciton

The dissociation energy of the charged exciton can be measured as the charged-exciton–neutral-exciton splitting at very low carrier density. At moderate carrier densities, it was found that the distance between the charged exciton and the neutral exciton varies with the carrier concentration. This variation has been studied in absorption experiments for both X^+ and X^- in CdTe-based QW's.^{22,23} It is linear with the density of carriers in the spin subband promoting the formation of the charged exciton. Similar results have been found for GaAs (Ref. 21) and ZnSe-based (Ref. 2) QW's.

In this work we have shown that the jump from the single X^+ line and the double $D_{high}-D_{low}$ lines, observed in σ^+ polarization, measures the binding energy of the charged exciton (the Zeeman splitting of the valence band at this field gives directly the zero-field splitting of the levels). This dissociation energy is plotted versus the carrier density in Fig. 15. No significant variation was observed, the splitting staying between 2 and 3 meV for all measured samples.

The apparent discrepancy between the line splitting in absorption spectra and this result of an analysis of the level crossing leads to the conclusion that in absorption, the system is left in an excited state that is at higher energy than the energy of the neutral exciton alone. This is in agreement with theoretical works^{24,25} that demonstrate that the increase of

the line splitting measured on the spectra is due to a transfer of oscillator strength to a high-energy tail of the exciton line, which contains exciton-carrier scattering states (or unbound states of the trion). Note that in the present study, we have an unambiguous determination of the binding energy of the charged exciton, but no real determination of the excited state, with respect to which this binding energy is measured. We simply know that this excited state contains holes all in the majority spin subband, and is close to the neutral exciton at low carrier density and to uncorrelated electron-hole pair at high carrier density.

VI. SUMMARY

We have studied a series of $\text{Cd}_{1-x}\text{Mn}_x\text{Te}$ QW's, with x below 0.01, containing a hole gas of density up to $5 \times 10^{11} \text{ cm}^{-2}$. In all samples, we observe either a dichroic line (one line in each of the σ^+/σ^- polarizations, with a splitting related to the giant Zeeman effect) at low values of the hole spin splitting, and a double line in σ^+ polarization only, at large spin splitting. In the first case, the spectra continuously emerge from the X^+ charged-exciton lines as the carrier density increases, and keep several characteristic features of the trion PL. In the other case, they resemble spectra due to band-to-band PL transitions.

The jump from the trionlike spectra to the double line is due to a crossing of the initial levels of the transitions. The charged exciton contains two holes arranged in a singlet state, which costs an energy equal to the hole spin splitting. When the hole spin is larger than the dissociation energy of the charged exciton, the charged exciton is destabilized in favor of a state where all holes are in the majority spin subband. We note that such large values of the spin splitting at low field can be achieved only in diluted magnetic semiconductors with a hole gas: In the case of an electron gas, at least four times larger Mn contents would have to be used. We find that the dissociation energy of the charged exciton coincides with the X/X^+ spectral splitting only at low carrier density. At moderate carrier density, the spectral splitting increases with the carrier density (in agreement with the results of theoretical studies which consider excitations accompanying the creation of the excitons), while the dissociation energy stays constant.

At very low spin splitting, the PL line and the absorption line do not coincide in energy ("excitonic Moss-Burstein shift"). This we ascribe to the fact that the position of the absorption line involves the creation of excitations of the hole gas in the presence of a charged exciton at Fermi wave vector, and that the position of the PL line involves excitations of the partially polarized hole gas resulting from the recombination of a charged exciton at the center of the Brillouin zone. Hence a new picture emerges from the present study for the neutral and charged excitons at moderate carrier density, with a constant binding energy of the trion, and various excitations of the hole gas involved in the transitions. The presence of this "excitonic Moss-Burstein shift" can be used to determine the carrier density (once a calibration has been performed), but also to determine the spin splitting that provokes the complete polarization of the hole gas. We ex-

perimentally find that, in the range of hole densities explored (from 0.5×10^{11} to $4 \times 10^{11} \text{ cm}^{-2}$), it increases with the carrier density, but remains smaller than the (doubled) Fermi energy. This enhancement of the spin susceptibility is by a factor at least larger than 2. However, in agreement with Kohn's theorem (which might not apply in the valence band), the observed spectroscopic splitting is not changed.

The double line observed in σ^+ polarization at a large-enough spin splitting displays several features of a band-to-band transition. The high-energy component D_{high} has the ground state as the final state, and it is associated with a strong LO-phonon replica: in a band-to-band picture, this involves an electron relaxed at $k=0$ in the conduction band recombining with a hole at Fermi wave vector in the valence band, so that the final state is the ground state. This transition, indirect in the reciprocal space, can be made to be slightly allowed by disorder and carrier-carrier interactions (Fermi edge singularity), but also by the creation of a phonon with a wave vector equal to k_F . The high-energy component D_{high} leaves some excitation in the carrier gas: in the band-to-band description, this final state corresponds to the excitation of a hole from $k=0$ to k_F , the single-particle energy being equal to $2E_F$ in our notation (i.e., the Fermi energy of the fully polarized hole gas). We note that this line is observed close to the energy extrapolated at zero field for the transitions between Landau levels, and also that a weak but distinct absorption line is seen in σ^+ polarization at complete hole polarization, with a shift with respect to the present lower component of the PL doublet nearly equal to the calculated Moss-Burstein shift. Hence the absorption line, the lower component of the double PL line, and the absorption lines at integer filling factors can be qualitatively understood in terms of electron-hole pairs.

However new features appear when a more quantitative description is attempted. The main discrepancy is the splitting between the two components of the double line. It is definitely larger than the Fermi energy (doubled since at full polarization) expected for the single-particle excitation promoting a hole from $k=0$ to k_F . This is particularly evident at intermediate carrier density while at the higher densities achieved, and considering the larger fluctuation of our data, it approaches the expected $2E_F$ value. As we have shown that the dynamics of the double line implies that a single initial state is involved, this energy has to be accounted for in terms of excitations of the hole gas (single-particle excitations or combinations of them, or plasmons, taking into account the effect of carrier-carrier interactions). The previous discussion of this double line as being close to a band-to-band transition suggests that the final state has a total wave vector equal to k_F .

ACKNOWLEDGMENTS

We wish to thank Ronald Cox, Vincent Huard, and Kuntheak Kheng for allowing us to use their experimental setup when installed at the Grenoble High Field Laboratory, and for numerous interesting discussions. This work is partially supported by the Polish-French Collaboration Program

Polonium, and by the Polish State Committee for Scientific Research (KBN grant No. 5 P03B 023 20). We thank also the Swiss National Research Foundation and the Federal Office

for Education and Science for partial support. This work would not have been possible without the strong contribution from the late André Wasiela.

*Electronic address: Piotr.Kossacki@fuw.edu.pl

- ¹K. Kheng, R.T. Cox, Y. Merle d'Aubigné, F. Bassani, K. Saminadayar, and S. Tatarenko, *Phys. Rev. Lett.* **71**, 1752 (1993).
- ²G.V. Astakhov, D.R. Yakovlev, V.P. Kochereshko, W. Ossau, W. Faschinger, J. Puls, F. Henneberger, S.A. Crooker, Q. McCulloch, D. Wolverson, N.A. Gippius, and A. Waag, *Phys. Rev. B* **65**, 165335 (2002).
- ³A. Esser, E. Runge, R. Zimmermann, and W. Langbein, *Phys. Rev. B* **62**, 8232 (2000).
- ⁴P. Redlinski and J. Kossut, *Solid State Commun.* **118**, 295 (2001).
- ⁵C. Riva, F.M. Peeters, and K. Varga, *Phys. Rev. B* **61**, 13873 (2000).
- ⁶B. Stébé, E. Feddi, A. Ainane, and F. Dujardin, *Phys. Rev. B* **58**, 9926 (1998) and references therein.
- ⁷G.V. Astakhov, V.P. Kochereshko, D.R. Yakovlev, W. Ossau, J. Nurnberger, W. Faschinger, G. Landwehr, T. Wojtowicz, G. Karczewski, and J. Kossut, *Phys. Rev. B* **65**, 115310 (2002).
- ⁸K. Kheng, *Ann. Phys. (Paris)* **20**, C2-229 (1995).
- ⁹S. Lovisa, R. T. Cox, N. Magnea, and K. Saminadayar, *Phys. Rev. B* **56**, R12787 (1997).
- ¹⁰G. Finkelstein, V. Umansky, I. Bar-Joseph, V. Ciulin, S. Haacke, J.-D. Ganière, and B. Deveaud, *Phys. Rev. B* **58**, 12637 (1998).
- ¹¹E. Vanelle, M. Paillard, X. Marie, T. Amand, P. Gilliot, D. Brinkmann, R. Lévy, J. Cibert, and S. Tatarenko, *Phys. Rev. B* **62**, 2696 (2000).
- ¹²H.W. Yoon, A. Ron, M.D. Sturge, and L.N. Pfeiffer, *Solid State Commun.* **100**, 743 (1996).
- ¹³P. Kossacki, V. Ciulin, M. Kutrowski, J.-D. Ganière, T. Wojtowicz, and B. Deveaud, *Phys. Status Solidi B* **229**, 659 (2002).
- ¹⁴M. Kutrowski, T. Wojtowicz, P. Kossacki, V. Ciulin, and J. Kossut, *Phys. Status Solidi B* **229**, 791 (2002).
- ¹⁵C.R.L.P.N. Jeukens, P.C.M. Christianen, J.C. Maan, D.R. Yakovlev, W. Ossau, V.P. Kochereshko, T. Wojtowicz, G. Karczewski, and J. Kossut, *Phys. Rev. B* **66**, 235318 (2002).
- ¹⁶V. Ciulin, P. Kossacki, S. Haacke, J.-D. Ganière, B. Deveaud, A. Esser, M. Kutrowski, and T. Wojtowicz, *Phys. Rev. B* **62**, R16310 (2000).
- ¹⁷P. Kossacki, V. Ciulin, M. Kutrowski, J.-D. Ganière, T. Wojtowicz, and B. Deveaud, in *Proceedings of the International Conference on Physics of Semiconductors*, Osaka, 2000 (Springer, Berlin, 2001), p. 623; V. Ciulin, P. Kossacki, M. Kutrowski, J.-D. Ganière, T. Wojtowicz, and B. Deveaud, *Phys. Status Solidi B* **229**, 627 (2002).
- ¹⁸S.A. Crooker, E. Johnston-Halperin, D.D. Awschalom, R. Knobel, and N. Samarth, *Phys. Rev. B* **61**, R16307 (2000).
- ¹⁹D. Sanvitto, D.M. Whittaker, A.J. Shields, M.Y. Simmons, D.A. Ritchie, and M. Pepper, *Phys. Rev. Lett.* **89**, 246805 (2002).
- ²⁰A. J. Shields, M. Pepper, M. Y. Simmons, and D. A. Ritchie, *Phys. Rev. B* **52**, 7841 (1995).
- ²¹B. Cole, T. Takamasu, K. Takehana, R. Goldhahn, D. Schulze, G. Kido, J.M. Chamberlain, G. Gobsch, M. Hemini, and G. Hill, *Physica B* **249–251**, 607 (1998).
- ²²V. Huard, R.T. Cox, K. Saminadayar, A. Arnoult, and S. Tatarenko, *Phys. Rev. Lett.* **84**, 187 (2000).
- ²³P. Kossacki, J. Cibert, D. Ferrand, Y. Merle d'Aubigné, A. Arnoult, A. Wasiela, S. Tatarenko, and J. A. Gaj, *Phys. Rev. B* **60**, 16018 (1999).
- ²⁴A. Esser, R. Zimmermann, and E. Runge, *Phys. Status Solidi B* **227**, 317 (2001).
- ²⁵R.A. Suris, V.P. Kochereshko, V.V. Astakhov, R.D. Yakovlev, W. Ossau, J. Nurnberger, W. Faschinger, G. Landwehr, T. Wojtowicz, G. Karczewski, and J. Kossut, *Phys. Status Solidi B* **227**, 343 (2001).
- ²⁶R.T. Cox, R.B. Miller, K. Saminadayar, and T. Baron, *Phys. Rev. B* **69**, 235303 (2004).
- ²⁷V. Huard, R.T. Cox, K. Saminadayar, C. Bourgognon, A. Arnoult, J. Cibert, S. Tatarenko, and M. Potemski, *Phys. Status Solidi A* **178**, 95 (2000).
- ²⁸T. Wojtowicz, M. Kutrowski, G. Karczewski, and J. Kossut, *Appl. Phys. Lett.* **73**, 1379 (1998).
- ²⁹V.P. Kochereshko, G.V. Astakhov, D.R. Yakovlev, W. Ossau, G. Landwehr, T. Wojtowicz, G. Karczewski, and J. Kossut, *Phys. Status Solidi B* **220**, 345 (2000).
- ³⁰O. Homburg, K. Sebald, P. Michler, J. Gutowski, H. Wensch, and D. Hommel, *Phys. Rev. B* **62**, 7413 (2000).
- ³¹C. Riva, F.M. Peeters, and K. Varga, *Phys. Rev. B* **63**, 115302 (2001).
- ³²A. Arnoult, D. Ferrand, V. Huard, J. Cibert, C. Grattapain, K. Saminadayar, C. Bourgognon, A. Wasiela, and S. Tatarenko, *J. Cryst. Growth* **201**, 715 (1999).
- ³³W. Maślana, M. Bertolini, H. Boukari, P. Kossacki, D. Ferrand, J. A. Gaj, S. Tatarenko, and J. Cibert, *Appl. Phys. Lett.* **82**, 1875 (2003).
- ³⁴A.J. Shields, J.L. Osborne, M.Y. Simmons, M. Pepper, and D.A. Ritchie, *Phys. Rev. B* **52**, R5523 (1995).
- ³⁵A.J. Shields, J.L. Osborne, M.Y. Simmons, D.A. Ritchie, and M. Pepper, *Semicond. Sci. Technol.* **11**, 890 (1996).
- ³⁶H. Boukari, P. Kossacki, M. Bertolini, D. Ferrand, J. Cibert, S. Tatarenko, A. Wasiela, J.A. Gaj, and T. Dietl, *Phys. Rev. Lett.* **88**, 207204 (2002).
- ³⁷A. Haury, A. Arnoult, V.A. Chitta, J. Cibert, Y. Merle d'Aubigné, S. Tatarenko, and A. Wasiela, *Superlattices Microstruct.* **23**, 1097 (1998).
- ³⁸A.A. Sirenko, T. Ruf, M. Cardona, D.R. Yakovlev, W. Ossau, A. Waag, and G. Landwehr, *Phys. Rev. B* **56**, 2114 (1997).
- ³⁹Q.X. Zhao, M. Oestreich, and N. Magnea, *Appl. Phys. Lett.* **69**, 3704 (1996).
- ⁴⁰V.P. Kochereshko, A.V. Platonov, D.R. Yakovlev, T. Wojtowicz, M. Kutrowski, G. Karczewski, J. Kossut, W. Ossau, and G. Landwehr, *Physica B* **256**, 557 (1998).
- ⁴¹T. Wojtowicz, M. Kutrowski, G. Karczewski, J. Kossut, F.J. Teran, and M. Potemski, *Phys. Rev. B* **59**, R10437 (1999).
- ⁴²J.A. Gaj, W. Grieshaber, C. Bodin-Deshayes, J. Cibert, G. Feuillet

- let, Y. Merle d'Aubigné, and A. Wasiela, Phys. Rev. B **50**, 5512 (1994).
- ⁴³Y. Shapira and N. F. Oliveira, Jr., Phys. Rev. B **35**, 6888 (1987).
- ⁴⁴U. Zehnder, B. Kuhn-Heinrich, W. Ossau, A. Waag, G. Landwehr, H.H. Cheng, and R.J. Nicholas, Acta Phys. Pol. A **90**, 989 (1996).
- ⁴⁵D. R. Yakovlev, V. P. Kochereshko, R. A. Suris, H. Schenk, W. Ossau, A. Waag, G. Landwehr, P.C.M. Christianen, and J.C. Maan, Phys. Rev. Lett. **79**, 3974 (1997).
- ⁴⁶Le Si Dang *et al.*, Solid State Commun. **44**, 1187 (1982).
- ⁴⁷G. Fishman, Phys. Rev. B **52**, 11132 (1995).
- ⁴⁸A. Lemaître, C. Testelin, C. Rigaux, T. Wojtowicz, and G. Karczewski, Phys. Rev. B **62**, 5059 (2000).
- ⁴⁹R. Planel, J. A. Gaj, and C. Benoît à la Guillaume, J. Phys. (Paris), Colloq. **41**, C5-39 (1980).
- ⁵⁰P. Kossacki, J. Phys.: Condens. Matter **15**, R471 (2003) and references therein.
- ⁵¹P. Kossacki *et al.*, in *Proceedings of the International Conference on Physics of Semiconductors*, Osaka, 2000 (Springer, Berlin, 2001), p. 623.
- ⁵²B. Jusserand, G. Karczewski, G. Cywiński, T. Wojtowicz, A. Lemaître, C. Testelin, and C. Rigaux, Phys. Rev. B **63**, 161302 (2001).
- ⁵³T. Jungwirth, B. Lee, and A.H. MacDonald, Physica E (Amsterdam) **10**, 153 (2001).
- ⁵⁴T. Dietl, A. Haury, and Y. Merle d'Aubigné, Phys. Rev. B **55**, R3347 (1997).
- ⁵⁵B.L. Altshuler and A.G. Aronov, in *Electron-Electron Interaction in Disordered Systems*, edited by A. L. Efros and M. Pollack (North-Holland, Amsterdam, 1985).
- ⁵⁶J. Zhu, H. L. Stormer, L. N. Pfeiffer, K. W. Baldwin, and K. W. West, Phys. Rev. Lett. **90**, 056805 (2003).
- ⁵⁷A. Haury, A. Wasiela, A. Arnoult, J. Cibert, T. Dietl, Y. Merle d'Aubigné, and S. Tatarenko, Phys. Rev. Lett. **79**, 511 (1997).